POLITECNICO
MILANO 1863

SCUOLA DI INGEGNERIA INDUSTRIALE
E DELL'INFORMAZIONE

Executive Summary of the Thesis

Numerical Study of Positron Production in Laser-Plasma Interaction with Double-Layer Targets via Non-linear Breit-Wheeler Process

Laurea Magistrale in Nuclear Engineering - Ingegneria Nucleare

Author: Leonardo Monaco

Advisor: Prof. Matteo Passoni

Co-advisors: Alessandro Maffini, Marta Galbiati

Academic year: 2022-2023

1. Introduction

The advent of laser facilities capable of generating extreme-intensity ($> 10^{22}\mathrm{W/cm^2}$) electromagnetic fields has opened up new frontiers in the interaction between light and matter. This includes the occurrence of strong-field Quantum Electrodynamics (QED) processes, notably the Non-linear Breit-Wheeler electron-positron Pair Production (NBWPP). The irradiation of materials by such light sources induces plasma formation, particle acceleration, and, among various types of radiation, the generation of positrons. The concept of a laser-driven NBWPP-based positron source has attracted considerable attention due to its potential unique properties, including high density, energy, and short duration, as well as low divergence and reduced retained radioactivity. Positron beams with these characteristics hold promise for a range of applications, such as particle colliders for fundamental research in physics, synchrotron radiation facilities for material characterization and medical imaging, positron annihilation spectroscopy for defect research, and laboratory astrophysics and plasma physics. Given the demanding nature in laser intensity of the NBWPP process, there is a keen interest in exploiting non-conventional targets to create conditions favorable for NBWPP while reducing the required laser intensity. Double-layer targets (DLTs), producible at Nanolab (Politecnico di Milano) laboratories, show great promise in this regard by offering the ability to optimize various aspects of their interaction with the laser. The thesis aims to investigate and characterize positron production through NBWPP using DLTs and a laser intensity available in experimental facilities [1], specifically $4.75 \times 10^{22}\mathrm{W/cm^2}$. Given the complexity of the problem, analytical tools are limited, necessitating a numerical approach. Simulations of the self-consistent dynamics of plasma populations and the electromagnetic field are employed, utilizing the particle-in-cell (PIC) method, chosen for its ability to unravel the intricate physics of the process at a relatively manageable computational cost. The selected laser intensity aligns with the goal of facilitating experimental validation of the simulation results in the present day. Due to the importance of accurately simulating positron production during laser-plasma interaction, a secondary objective of this thesis, within the Honours Programme, is to analyze the performance and limitations of the adopted simulation tool.

2. Fundamentals

NBWPP is a non-linear process where a photon, interacting with an intense electromagnetic field, can convert into an electron-positron ($e^- - e^+$) pair [2]. The probability and properties of the produced pair are governed by the photon quantum parameter, dependent on the photon energy $\mathcal{E}_\gamma$ and velocity $\boldsymbol{v} = \boldsymbol{c}$, and defined as:

$$\chi_\gamma = \frac{\mathcal{E}_\gamma}{E_s m_e c^2} \sqrt{\left(\boldsymbol{E} + \frac{\boldsymbol{v}}{c} \times \boldsymbol{B}\right)^2 - \left(\frac{\boldsymbol{v} \cdot \boldsymbol{E}}{c}\right)^2} \quad (1)$$

where $E_s \simeq 1.32 \times 10^{18}$ V/m is the Schwinger field, m_e is the electron mass, c is the speed of light, and $\boldsymbol{E}$ and $\boldsymbol{B}$ are the electric and magnetic field components. Assuming the pair particles as ultra-relativistic and emitted collinearly with the photon, the energy conservation law $\mathcal{E}_\gamma = \mathcal{E}_+ + \mathcal{E}_-$ holds, meaning the distribution of photon energy within the pair. The total probability rate of the process exhibits a threshold dependence on χ_γ, vanishing rapidly when $\chi_\gamma \ll 1$, and becoming significant as χ_γ, dependent on photon energy, field magnitude, and interaction geometry between $\boldsymbol{c}$, $\boldsymbol{E}$, and $\boldsymbol{B}$, approaches unity. This emphasizes the importance of having energetic photons ($\mathcal{E}_\gamma \gg m_e c^2$) and an optimal interaction geometry to alleviate laser intensity requirements. This condition is attained when the laser counterpropagates relatively to photons. A similar process occurring in intense fields is high-energy photon emission by a relativistic electron [2], known as Non-linear Inverse Compton Scattering (NICS). The quantum parameter χ_e for the emitting electron can be introduced similarly to eq. (1), but by substituting the electron energy $\mathcal{E}_e$ and velocity $\boldsymbol{v}$. It is enhanced by high electron energies and optimized interaction geometry between $\boldsymbol{v}$, $\boldsymbol{E}$, and $\boldsymbol{B}$, as discussed previously. Efficient high-energy photon emission occurs as χ_e approaches unity. Assuming the electron is ultra-relativistic and the emission is collinear, the equation $\mathcal{E}_e = \mathcal{E}_{e'} + \mathcal{E}_\gamma$ holds for the photon and electron before (e) and after (e') the emission, directly accounting for radiation reaction.

After defining the favorable conditions for NBWPP, these must be met during laser interaction with a target—specifically, a laser pulse with frequency w and peak intensity I interacting with the DLT. Several intermediate processes contribute to achieving the conditions for pair production, including electron acceleration, laser reflection, and photon emission. The DLT is composed of a low-density (few mg/cm^3) layer, a dozen of μm long, deposited on a metallic, solid-density film that is few μm thick. Initially, the target is ionized by the leading edge of the pulse, forming a plasma. The low-density layer, realized through pulsed laser deposition [3], features a near-critical electron density n_e satisfying $n_c < n_e < \gamma_0 n_c$, where $n_c = m_e w^2/(4\pi e^2)$ is the critical density in Gaussian units, $\gamma_0 = \sqrt{1 + a_0^2/2}$ is the relativistic factor, $a_0 = e\sqrt{8\pi I}/(m_e w c^{3/2})$ is the normalized vector potential, and e is the fundamental charge. In this regime, the laser pulse can propagate within the first layer of the DLT, creating a channel of depleted electrons through the ponderomotive force [4], arising from the non-uniformity of laser intensity. During this phase, some electrons become trapped within the channel and, while co-moving with the laser pulse and undergoing relativistic oscillations, absorb energy from the laser via Direct Laser Acceleration (DLA) [5]. Although photons are emitted during this phase, they are not capable of undergoing NBWPP. The near-critical density, compared to an under-dense gas, improves electron heating, generating a larger number of energetic electrons. On the channel axis, the depleted electron concentration and their rapid oscillations result in a higher index of refraction, acting as a lens [4]. This focusing effect leads to a reduction in the pulse's transverse size, thereby increasing the peak intensity. Meanwhile, ions exhibit much slower dynamics than electrons due to the larger inertia, and can be considered almost immobile [4]. The thin metallic layer features an over-dense electron density ($n_e > \gamma_0 n_c$), implying that when the pulse reaches this layer, cannot propagate within it and is instead reflected. This step is crucial, since the laser intensity is enhanced by superposition of the incident and reflected components, and the latter also provides the optimal interaction geometry for NICS and NBWPP. The hot electrons, when interacting with the reflected laser field, emit energetic photons, which, in turn, interact with the same field and can undergo NBWPP, producing positrons. A schematic view of laser-DLT interaction phases and positron emission is illustrated in Figure 1.

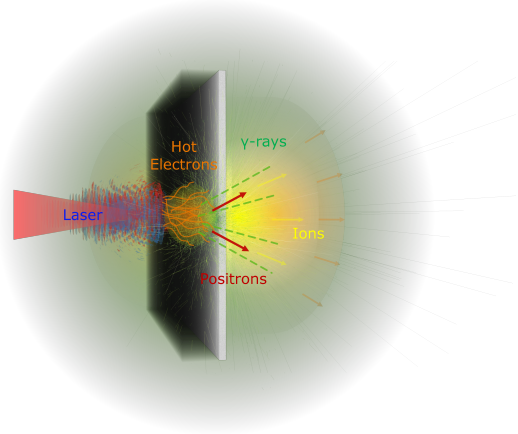

Figure 1: Diagram of laser-DLT interaction phases: laser impinging on the DLT, electron acceleration, photon emission, and positron production. The diagram indicates the directions of emission for photons and positrons.

To capture all the physics, including the accurate modeling of single-particle processes such as NICS and NBWPP, a kinetic plasma description is necessary. An analytical solution to such a problem is generally not feasible. Therefore, a numerical approach is required, and the PIC method [4] is one of the most widely used. The PIC method adopts a particle description to approximately solve the collision-less relativistic kinetic Maxwell-Vlasov system of equations [4]. The plasma particles are represented by a reduced number of numerical particles with arbitrarily chosen spatial extension and a unique velocity. The spatial domain is discretized into a grid, and at each time step, numerical particles move across it under the action of the self-consistent electromagnetic field through the Lorentz force. Their motion follows the solution of relativistic Newton equations. The particles deposit charge and current densities on the grid, contributing to the source terms in Maxwell equations for updating the electromagnetic field. Photon emission via NICS and pair production through NBWPP are modeled by an additional Monte Carlo (MC) module. At each time step, the occurrence of processes, described as collinear, and the energy of secondary particles are determined by MC calculations. When an event occurs, after the creation of a numerical photon or pair, the emitting electron or the converted photon, respectively, is appropriately updated. A controllable MC parameter influencing the statistics of NBWPP simulation is the photon sampling, which sets the number of numerical photons generated at each emission event while conserving the total number of represented real photons.

3. Objectives and Methods

The primary objective of this thesis is to numerically investigate the physics of NBWPP during laser-plasma interaction in DLT targets, along with the characterization of the produced positrons. Additionally, an exploration of the main DLT parameters is conducted to optimize positron production for the potential realization of a positron beam source. This study aims to provide insights into the feasibility of an NBWPP-based positron beam source by using a DLT and lasers currently available in experimental facilities. The adopted laser parameters include a wavelength of 0.8 μm, peak intensity of $4.75 \times 10^{22}\mathrm{W/cm}^2$, linear polarization, spot size of 3 μm, and temporal duration of 30 fs. Furthermore, this work seeks to confirm the potentialities of the considered source regarding positron beam features. These objectives are pursued using SMILEI, an open-source, highly parallelized PIC code integrated with a MC module for the modeling of NICS and NBWPP. As a secondary objective, in quality of Honours Programme additional thesis activity, an analysis of the MC module's capability to accurately simulate NBWPP is conducted. 2D simulations are employed as a reasonable trade-off to capture the interesting physics while mitigating simulation run-time. Given the intensive computational demands of the simulations, they are performed on supercomputers, specifically the Galileo100 cluster hosted by CINECA (Bologna).

4. Results and discussion

To explore the physics of NBWPP in DLTs and analyze the MC module, 2D simulations of a laser pulse striking a carbon low-density ($n_e = 2n_c$) layer, 15 μm in length, attached to a 1 μm thick aluminum ($n_e = 450n_c$) foil, are performed. The laser's electric and magnetic fields oscillate along the y-axis and z-axis, respectively. As the laser pulse propagates within the DLT's first layer (100 fs $< t <$ 170 fs), two mechanisms come into play: electron heating and the focusing of the laser pulse. Despite a reduction in

the total energy of field components due to absorption by electrons, the net effect, as shown in Figure 2, is an increase in their amplitude and, consequently, in peak intensity. While ions remain almost immobile due to their inertia, electrons are pushed in the forward and radial directions by the laser ponderomotive force producing charge separation, which results in quasi-static longitudinal (E_x) and transverse (E_y) electric fields. As the pulse reaches the metallic foil, reflection begins, marked by a substantial enhancement in the field components' amplitude, almost doubling their value. This corresponds to a significant boost in laser intensity in the superposition region. During reflection, E_x is also significantly enhanced, indicating the formation of the Target Normal Sheath Acceleration (TNSA) field [4]. This longitudinal field is formed on the rear side of the target, where hot electrons escape separating from positive ions.

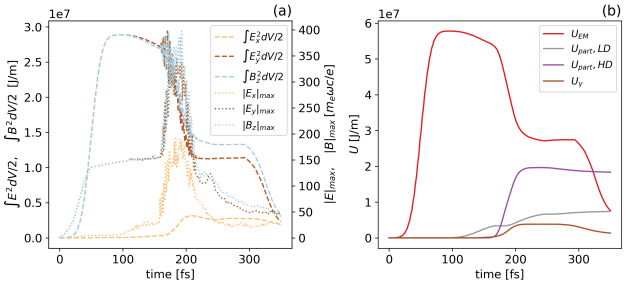

Figure 2: Time evolution of the total energy and maximum values of the relevant components of the electromagnetic field (a) and the total energy of the field and plasma populations (b), including particles of the low-density (LD) and high-density (HD) layers of the DLT, and photons.

At reflection onset, electrons exhibit energies surpassing 700 MeV, and their interaction with the field in the superposition region enhances their quantum parameter, reaching values around 0.8. Throughout the reflection period, electrons emit photons via NICS with energies and quantum parameters extending up to 450 MeV and above 0.6, respectively. The corresponding electron and photon spectra are reported in Figure 3. Within the same time-frame and spatial region, these photons have relevant probability of converting into pairs through NBWPP. The trajectories of produced positrons and electrons are shown in Figure 4, spanning from their creation to the conclusion of laser-DLT interaction when the reflected laser pulse exits the target. The majority of positrons are accelerated in the forward direction by the TNSA field, forming a beam, while electrons are slowed down and cannot escape from the target.

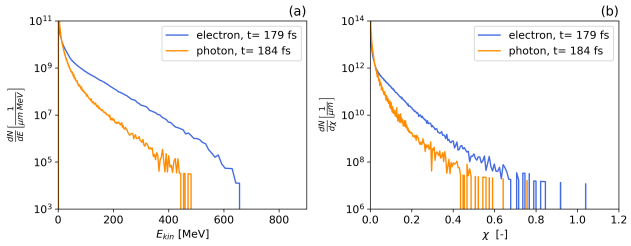

Figure 3: Electron and photon spectra in terms of kinetic energy (a) and quantum parameter (b). The spectra are evaluated at the onset of reflection for electrons, while during reflection for photons.

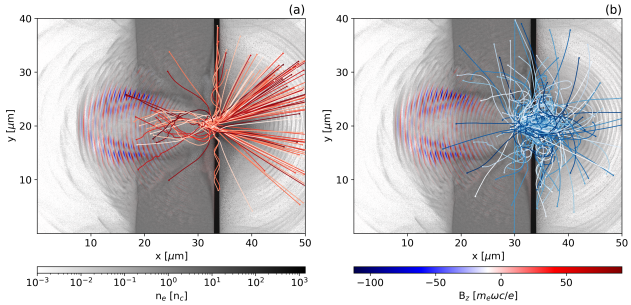

Figure 4: Trajectories of positrons (a) and electrons (b) from their generation via NBWPP to conclusion of laser-DLT interaction. The DLT is visualized by its electron density, while the laser pulse through the B_z component.

A crucial aspect revealed by the analysis pertains to the reflectivity of the substrate. During reflection, the laser pulse partially penetrates the substrate foil, depositing its energy through electron and ion heating. As shown in Figure 2, almost one-third of the total laser energy is deposited, reducing the available intensity for NBWPP in the superposition region. This indicates a poor reflectivity of the aluminum foil. Therefore, an analysis considering four different substrates is conducted, independently varying the density ($n_e = 100n_c$), the atomic mass (A=197) and the thickness (5 μm). The resulting fraction of laser energy converted into pairs is reported in Figure 5 (a). It emerges that density and atomic mass play a central role in reflectivity; higher values for both decrease the energy depo-

sition within the substrate and enhance the laser intensity in the superposition region, leading to a larger number of pairs produced. Concerning thickness, adopting few micrometers instead of one shows to be beneficial for reflectivity and pair production, without deteriorating the formation of the TNSA field.
Subsequently, a parametric analysis of the density and length of the low-density layer is performed, and the configurations investigated, along with the fraction of laser energy converted into pairs, are illustrated in Figure 5 (b). It emerges that the properties of the low-density layer strongly influence the electron acceleration phase, laser focusing effect, and laser energy absorption. The results of the analysis indicate that, among the parameters explored, an optimal configuration exists. The low-density layer with density of $n_e = 2n_c$ and length of 39 μm not only provides the best performance in terms of laser-to-positron energy conversion efficiency, but also in relation to positron beam features.

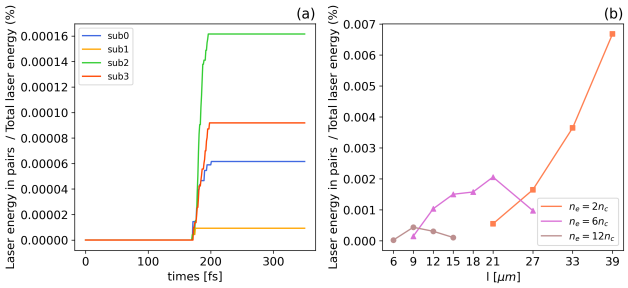

Figure 5: In panel (a), the fraction of laser energy converted into pairs, considering a $n_e = 2n_c$ dense and 15 μm long low-density layer attached to different substrate foils. The 1 μm thick, aluminum (A=27, $n_e = 450n_c$) foil is indicated as "sub0", while in "sub1", "sub2", "sub3" one property is varied, specifically $n_e = 100n_c$, A=197, and thickness of 5 μm, respectively. In panel (b), the fraction of laser energy converted into pairs, considering different densities and lengths for the low-density layer attached to a 2 μm thick, lead (A=207, $n_e = 568n_c$) foil.

Considering the optimal configuration for the low-density layer, attached to a 2 μm thick lead substrate, a beam populated by $4.5\times10^7 1/\mu$m positrons per unit length is obtained. Its angular distribution, peaking at $\pm25°$, and energy spectrum are reported in Figure 6. The beam features a divergence of 28°, temporal duration of 19.6 fs, and average density of 4.4×10^{17} cm^{-3}. The energy spectrum peaks at 342 MeV and extends up to 800 MeV, exhibiting an energy spread of 215 MeV. The fraction of laser energy converted into pairs and the laser-to-positron energy conversion efficiency are, respectively, 0.007% and 0.005%.

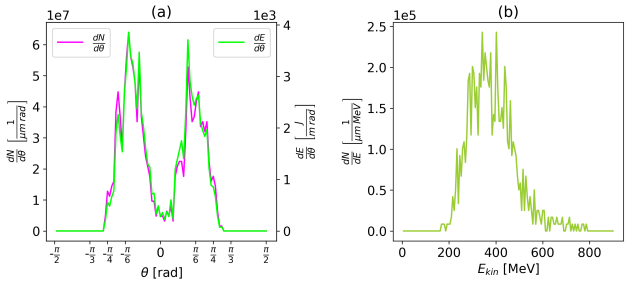

Figure 6: Angular distribution in particle number and energy (a) and energy spectrum (b) of the produced positron beam for the optimal configuration of the DLT, featuring a $n_e = 2n_c$ dense and 39 μm long low-density layer attached to a lead foil.

From the analysis of the MC module for NBWPP simulation, various criticalities and limits emerge. Firstly, the limitation in statistics arising from the PIC description adopting a restricted number of numerical particles is confirmed. As shown, for instance, in Figure 3, the tails of the spectra, representing particles with highest energy and quantum parameter, are not simulated. Regarding the photon sampling parameter, when the number of NBWPP events is small due to suboptimal conditions, it must be carefully chosen to avoid numerical noise affecting physical quantities, such as the energy converted into positrons. Out of this case, the photon sampling does not affect physical quantities but only the number of numerical positrons produced, and consequently, the statistics for the characterization of real positrons. Considering the positron generation spectrum and energy converted into pairs, a comparison between simulation results and theoretical predictions is performed and reported in Figure 7, showing good accordance when a sufficient number of numerical particles is produced. A test of theoretical assumptions involved in the modeling of NBWPP and NICS is also conducted, demonstrating that they are abundantly satisfied at the considered laser intensity. However, some numerical

approximations involved in the implementation of the processes lead to momentum and energy non-conservation along the simulation.

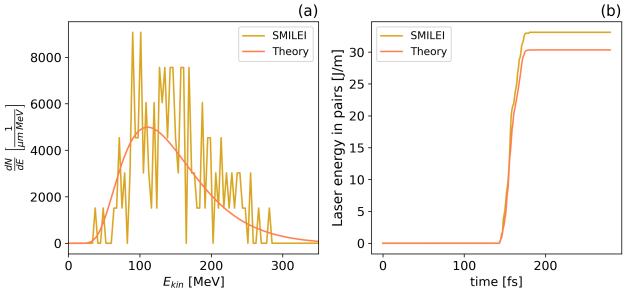

Figure 7: Comparison between simulation results and theoretical predictions for the positron generation spectrum (a) and energy converted into pairs (b). The DLT considered consists of a 15 μm long low-density ($n_e = 2n_c$) layer attached to an 1 μm thick slab of aluminum.

5. Conclusions and perspectives

Driven by the unique properties and interesting applications of a NBWPP-based positron beam source, the goal of this thesis is to explore the potential of producing positron beams through NBWPP using DLTs and a laser intensity available in current experimental facilities. The investigation reveals crucial phases in the process, including electron acceleration to energies exceeding several hundreds of MeV, laser field focusing and reflection, and its interaction with accelerated electrons and subsequently produced photons. These phases are strongly influenced by DLT properties, in particular the analysis indicates the superior performance of DLTs formed by a micrometer-thick, dense, heavy substrate like lead, paired with a low-density layer featuring $n_e = 2n_c$ and a length around 39 μm. A notable advantage of DLTs is the TNSA field, which selectively accelerates positrons while decelerating electrons, resulting in a high-purity positron beam. In conclusion, the DLT configuration allows for the generation of a significant number of positrons at the considered laser intensity, reinforcing the interest in further exploring NBWPP in DLTs. The results also confirm the expected orders of magnitude of positron beam features for NBWPP-based sources, which represent the advantages over other sources, specifically in terms of temporal duration, average density, and positron spectrum. Future perspectives include further investigation of unexplored DLT parameters, the extension of the numerical study to 3D simulations to examine three-dimensionality effects, and the design of an experimental campaign at existing laser facilities like ELI to validate the obtained results. Experimental validation is essential to establish the feasibility of the investigated positron source.
The MC module in general provides satisfactory results in simulating NBWPP. However, there are specific cases where poor statistics, resulting from a limited number of secondary particles produced, can introduce numerical noise affecting physical quantities. Statistics limitations impacting the tails of the spectra, inherent in the PIC description, are unavoidable. This is expected to influence significantly processes affected by these tails, such as NBWPP. Additionally, numerical approximations lead to the non-conservation of energy and momentum. However, further studies are required to assess the physical significance of this non-conservation, especially as the number of events increases, as expected in laser-plasma interaction regimes accessible in future with the advent of the next generation multi-PW class lasers.

References

[1] J. W. Yoon, Y. G. Kim, W. I. Choi, J. H. Sung, H. W. Lee, S. K. Lee, and C. H. Nam. Realization of laser intensity over 1023 w/cm2. *Optica*, 2021.

[2] Ritus. Quantum effects of the interaction of elementary particles with an intense electromagnetic field. *Journal of Soviet Laser Research volume*, 1985.

[3] A. Zani, D. Dellasega, V. Russo, and M. Passoni. Ultra-low density carbon foams produced by pulsed laser deposition. *Carbon*, 2013.

[4] A. Macchi. *A Superintense Laser–Plasma Interaction Theory Primer*. Springer, 2013.

[5] M. Jirka, M. Vranic, T. Grismayer, and L. O. Silva. Scaling laws for direct laser acceleration in a radiation-reaction dominated regime. *New Journal of Physics*, 2020.